Article

Dissection, Optimization and Structural Analysis of a Covalent Irreversible DDAH1 Inhibitor

Gayle Burstein-Teitelbaum, Joyce Er, Arthur F. Monzingo, Alfred Tuley, and Walter Fast

Biochemistry, **Just Accepted Manuscript** • DOI: 10.1021/acs.biochem.8b00554 • Publication Date (Web): 08 Jul 2018

Dissection, Optimization and Structural Analysis of a Covalent Irreversible DDAH1 Inhibitor

*Gayle Burstein-Teitelbaum,[†] Joyce A.V. Er,[†] Arthur F. Monzingo,[‡] Alfred Tuley,[†] Walter Fast[†,]**

[†]Division of Chemical Biology & Medicinal Chemistry, College of Pharmacy, University of Texas, Austin, TX 78712, United States

[‡]Center for Biomedical Research Support, University of Texas, Austin, TX 78712, United States

ABSTRACT

Inhibitors of the human enzyme dimethylarginine dimethylaminohydrolase-1 (DDAH1) can control endogenous nitric oxide production. A time-dependent covalent inactivator of DDAH1, N^5-(1-imino-2-chloroethyl)-L-ornithine (K_I = 1.3 μM, k_{inact} = 0.34 min^{-1}), was conceptually dissected into two fragments and each characterized separately: L-norvaline (K_i = 470 μM) and 2-chloroacetamidine (K_I = 310 μM, k_{inact} = 4.0 min^{-1}). This analysis suggested that the two fragments were not linked in a manner that allows either to reach full affinity or reactivity, prompting the synthesis and characterization of three analogs: two that mimic the dimethylation status of the substrate, N^5-(1-imino-2-chloroisopropyl)-L-ornithine (k_{inact}/K_I = 208 $M^{-1}s^{-1}$) and N^5-(1-imino-2-chlorisopropyl)-L-lysine (k_{inact}/K_I = 440 $M^{-1}s^{-1}$), and one that lengthens the linker beyond that found in the substrate, N^5-(1-imino-2-chloroethyl)-L-lysine (Cl-NIL, K_I = 0.19 μM, k_{inact} = 0.22 min^{-1}). Cl-NIL is one of the most potent inhibitors reported for DDAH1, inactivates with a second order rate constant (1.9×10^4 $M^{-1}s^{-1}$) larger than the catalytic efficiency of DDAH1 for its endogenous substrate (1.6×10^2 $M^{-1}s^{-1}$), and has a partition ratio of 1 with a >100,000-fold selectivity for DDAH1 over arginase. An activity-based protein-profiling probe is used to show inhibition of DDAH1 within cultured HEK293T cells (IC_{50} = 10 μM), with cytotoxicity only appearing at higher concentrations (ED_{50} = 118 μM). A 1.91 Å resolution X-ray crystal structure reveals specific interactions made with DDAH1 upon covalent inactivation by Cl-NIL. Dissecting a covalent inactivator and analysis of its constituent fragments proved useful for the design and optimization of this potent and effective DDAH1 inhibitor.

INTRODUCTION

Nitric oxide biosynthesis is highly regulated to preserve the function of this second messenger in biological signaling by neuronal and endothelial nitric oxide synthases, and to unleash the toxicity of this radical when overproduced by inducible nitric oxide synthase.[1] One atypical control mechanism used is the direct inhibition of these three nitric oxide synthase isoforms by endogenously produced methylarginines.[2] Both asymmetric N^{ω},N^{ω}-dimethyl-L-arginine (ADMA) and N^{ω}-monomethyl-L-arginine (NMMA) are released by proteolysis of posttranslationally modified proteins, and these methylarginines play functional roles in their "second act" as a reversible inhibitor (ADMA, Figure 1) or an irreversible inactivator (NMMA) of nitric oxide synthase.[3-10] Both ADMA and NMMA are present in plasma at low micromolar / high nanomolar concentrations in healthy persons, are elevated in disease states such as in patients with chronic renal disease, and regulate vascular tone through inhibition of nitric oxide production in the endothelium.[11] The concentrations of these inhibitory methylarginines are controlled by both renal excretion and metabolism, with the main catabolic enzyme for both being dimethylarginine dimethylaminohydrolase-1 (DDAH1).[11, 12]

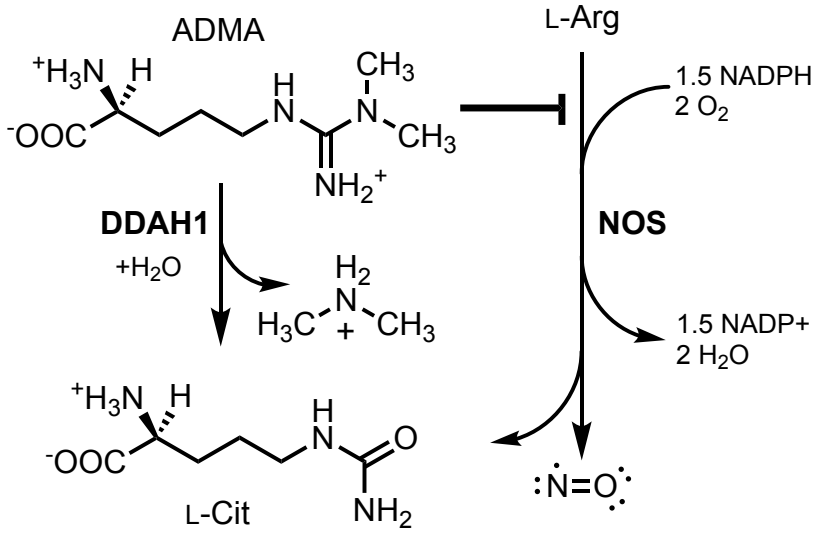

Figure 1. Regulation of •NO Production by DDAH1. Conversion of L-Arg to •NO by isoforms of NOS is inhibited by endogenously produced ADMA, the concentrations of which are regulated by DDAH1 activity.

Pharmacologically-useful inhibitors of DDAH1 can be of potential benefit to pathologies with elevated nitric oxide production by preventing catabolism of methylarginines and enhancing their ability to inhibit nitric oxide synthases.[2] Examples include DDAH1 inhibitors that regulate vascular tone, that improve survival in models of septic shock, and that reduce collagen deposition and epithelial proliferation in idiopathic pulmonary fibrosis.[13-15] DDAH1 is also upregulated in melanomas (and other cancers) and likely serves to enhance nitric oxide production, which correlates with poor patient survival.[16-19] Potent and selective inhibitors of DDAH1 are of use as biochemical tools for elucidating the role of this enzyme in pathological states, and for potential therapeutic development.[20] We previously reported a covalent inactivator of DDAH1, N^5-(1-imino-2-chloroethyl)-L-ornithine (Cl-NIO) and demonstrated its ability to target DDAH1 expressed within cultured cells and to selectively inhibit nitric oxide production in a melanoma cell line with upregulated DDAH1.[16] Herein, we describe the optimization of this inhibitor by dissecting the compound into two fragments, and characterizing each fragment individually. The stepwise characterization of these fragment components led to non-obvious improvements resulting in reconstruction of a very potent and selective inactivator with cellular availability as a promising probe for DDAH1 study.

MATERIALS AND METHODS

Expression and purification of human DDAH1

Wild-type human DDAH1 bearing an *N*-terminal His_6 affinity tag was expressed using an expression plasmid encoding a reengineered *N*-terminus (pET28a-hDDAH-1re) to avoid *N*-terminal nonenzymatic gluconylation, as described previously.[21] Briefly, recombinant His_6-DDAH1 was purified after expression in *E. coli* BL21(DE3) by affinity and hydrophobic interaction chromatography according to the previous procedure[21] with the following modifications: Elution Buffer (25 mL) (50 mM NaH_2PO_4, 300 mM NaCl, 250 mM imidazole, 15% glycerol pH 8.0) was used to elute protein from the Ni-NTA affinity resin (8mL, Qiagen). The eluent was diluted into Buffer A (50 mM NaH_2PO_4, 3.0 M NaCl, 15 % glycerol, pH 7.0) to a final NaCl concentration of 1.8 M and loaded onto a 1.5 × 18 cm phenyl-sepharose column (GE Healthcare, Piscataway, NJ). Proteins were eluted using a stepwise gradient of Buffer A supplemented with 1.8 M NaCl, and subsequent steps with 1.6 M, 1.3 M, and 1M NaCl. As gauged by SDS-PAGE, fractions containing DDAH1 were pooled and concentrated using an Amicon Centrifugal Filter (Millipore, Billerica, MA) with a 10 kDa molecular weight cutoff. The final protein was dialyzed overnight in Dialysis Buffer 1 (2 mM 1,10-phenanthroline, 100 mM KCl, 10 % glycerol, pH 7.3) followed by 2 × 4 h dialyses in Chelex-100 (BioRad) treated Dialysis Buffer 2 (50 mM KH_2PO_4, 100 mM KCl, 10 % glycerol, pH 7.3), flash frozen and stored in aliquots at -80 ºC. All buffers were made using deionized water.

Synthetic Methods

A general synthetic scheme is provided in Supporting Information (Figure S1) to illustrate the transformations described below.

2-Chloroethanimidic acid, ethyl ester: Chloroacetonitrile (2.55 mL, 40.3 mmol) and anhydrous ethanol (2.6 mL, 22.4 mmol) were added to 22 mL of anhydrous diethyl ether and cooled to 0 °C. The solution was bubbled through with $HCl_{(g)}$ until a white precipitate formed. The precipitate was washed with cold diethylether followed by cold hexanes to yield 2-chloroethanimidic acid, ethyl ester, HCl (1.8 g, 78 %). ^{1}H-NMR (300 MHz, D_2O): 4.66 (2 H, overlapped with reference peak), 4.16 (2 H, s), 1.16 (3 H, d, J = 7.2 Hz).

2-Chloropropanimidic acid, ethyl ester: Chloropropionitrile (3.5 mL, 39.56 mmol) and anhydrous ethanol (2.6 mL, 22.4 mmol) were added to 20 mL of anhydrous diethylether and cooled to 0 °C. The solution was bubbled through with $HCl_{(g)}$ until a white precipitate formed. The precipitate was washed with cold diethyl ether followed by cold hexanes to yield 2-chloropropanimidic acid, ethyl ester, HCl. (1.4 g, 46 %). ^{1}H-NMR (400 MHz, D_2O): 4.10 (1 H, q, J = 7.6 Hz), 3.19 (2 H,m), 1.48 (3 H, dd, J_1 = 6.8 Hz, J_2 = 22.8 Hz), 1.07-1.15 (3 H, m).

General methods for synthesis of chloroamidine inactivators: N^{α}-(*Tert*-butoxycarbonyl)-L-ornithine or N^{α}-(*t*-butoxycarbonyl)-L-lysine (1 mmol of either) was dissolved in 5 mL water at 0 °C followed by the dropwise addition of 2.5 M NaOH to bring the pH to 10. Either 2-chloroethanimidic acid methyl ester or 2-chloropropanimidic acid methyl ester was added in portions (2.5 mmol final), keeping the reaction at pH 10 through dropwise addition of NaOH. After addition of either of the imidic acids was completed, the reaction was stirred at 0 °C for 2 h and at room temperature for 1 additional hour. The reaction was neutralized by the dropwise addition of 1 M HCl and stirred at 4 °C for 1.5 days. Volatile solvents were removed by reduced pressure rotary evaporation and the resulting compound was purified using a Teledyne/Isco CombiFlash Rf200 Redi*Sep* Rf 26 g C18 Reverse Phase column (0.1 % TFA/H_2O to 0.1 % TFA/MeOH linear gradient) at the Texas Institute for Drug and Diagnostic Development

(University of Texas at Austin). Volatile solvents were removed by reduced pressure rotary evaporation and the remaining residue treated with 4 M HCl in 1,4-dioxane for 2 h to remove the *t*-Boc protecting group. Volatile solvents were removed as above to yield the desired products.

N^6-(1-Imino-2-chloroethyl)-L-lysine, HCl (Cl-NIL) ^{1}H-NMR (400 MHz, D_2O): 4.26 (2 H, s), 3.87 (1 H, t, J = 6 Hz), 3.22 (2 H, t, J = 7.2 Hz), 1.80-1.84 (2 H, m), 1.57-1.60 (2 H, m), 1.38-1.47 (2H, m). ^{13}C-NMR(D_2O): 171.58, 162.19, 52.24, 41.64, 38.61, 28.75, 25.51, 21.0. ESI (*m/z*) M + H^+ calcd for $C_8H_{17}ClN_3O_2$, 222.10038; found 222.10029.

N^6-(1-Imino-2-chloroisopropyl)-L-lysine, HCl (Me-Cl-NIL) ^{1}H-NMR (400 MHz, D_2O): 4.68 (1 H, overlapped with reference peak), 3.831 (1 H, t, J = 6.2 Hz), 3.188 (2 H, t, J = 7.2 Hz), 1.25-1.91(9 H, m). ^{13}C-NMR(D_2O): 172.54, 166.21, 53.07, 51.63, 42.06, 29.38, 26.0, 22.04, 21.53. ESI (*m/z*) M + H^+ calcd for $C_9H_{19}ClN_3O_2$, 236.11603; found 236.11632.

N^5-(1-Imino-2-chloroisopropyl)-L-ornithine, HCl (Me-Cl-NIO) ^{1}H-NMR (400 MHz, D_2O): 4.70 (1 H, overlapped with reference peak), 3.95 (1 H, t, J = 6.4 Hz), 3.241 (2 H, t, J = 6.8 Hz), 1.63-1.94 (6 H, m), 1.61 (3 H, d, J = 7.2 Hz). ^{13}C-NMR(D_2O): 172.44, 166.73, 53.06, 51.89, 41.95, 27.32, 22.63, 22.04. ESI (*m/z*) M + H^+ calcd for $C_8H_{17}ClN_3O_2$, 222.10031; found 222.10023.

The activity-based protein profiling probe CAA-probe (*N*-but-3-ynyl-2-chloroacetamidine) was synthesized as previously described, as was the inactivator Cl-NIO (N^5-(1-imino-2-chloroethyl)-L-ornithine).[16, 22] Unless specified otherwise, all other chemicals were from the Sigma Aldrich Chemical Co. (St. Louis, MO).

Time-dependent inactivation kinetics

Purified His_6-DDAH1 (60 – 100 nM) was incubated with inactivators (Cl-NIL, Cl-NIO, Me-Cl-NIL, or Me-Cl-NIO) (0-64 μM) in Reaction Buffer (100 mM KH_2PO_4, 100 mM KCl, 2 mM EDTA, 1 % Tween-20, pH 7.3). To test for time-dependent loss of activity, aliquots were removed from the incubations at time points (0-60 min) and diluted two-fold into an assay solution containing a large excess (300 μM) of the alternative substrate, *S*-methyl-L-thiocitrulline (SMTC, Figure S2, K_M = 15 μM).[23] The remaining enzyme activity was assayed by detecting methanethiol release upon substrate hydrolysis using 7-diethylamino-3-(4'-maleimidylphenyl)-4-methylcoumarin (CPM), as described elsewhere.[24-26] The percent remaining activity across the experimental timescale was fitted to a single exponential to determine the observed inactivation rate at each concentration (k_{obs}). The plot of k_{obs} values versus inhibitor concentration was fitted to a quadratic equation for tight binding to give K_I if the enzyme and inhibitor concentrations were similar [k_{obs}=R((([E]+[I]+K_I)-(([E]+[I]+K_I)^2-(4[E][I]))$^{1/2}$)/2[E]), letting R and K_I float].[27, 28] If the inhibitor concentrations were well above that of the enzyme, the k_{obs} values versus inhibitor concentration plot was fitted instead to a non-linear version of the Kitz and Wilson plot to determine K_I and k_{inact} values.[29]

IC_{50} determination with DDAH1

To determine whether purified DDAH-1 is inhibited by L-Nva, purified His_6-DDAH1 (4 μM) was incubated with varying concentrations of L-Nva (50 μM – 10 mM) in the presence of ADMA (340 μM), KCl (100 mM), K_2HPO_4 buffer (100 mM), EDTA (5 mM) and Tween-20 (0.02%) at pH 7.4, for 45 min at 25 °C. The reaction was quenched with 10 μL of trichloroacetic acid (6 M) and the formation of the L-citrulline product was determined using a color developing reagent (COLDER assay) which detects compounds containing urea functional groups, as described previously.[30] The IC_{50} value and Hill coefficient (h) were fitted using

Activity(%)=(100/(100/(1+(IC_{50}/[L-Nva])^h))) and the K_i value calculated by the method of Cheng and Prusoff, assuming competitive inhibition and using a K_M for ADMA of 170 μM.[23, 31]

Partition ratio determination

To determine the partition ratio of DDAH1 inactivation by Cl-NIL, purified His_6-DDAH1 (62 nM) was incubated with varying concentrations (substoichiometric to suprastoichometric) of Cl-NIL (0-400 nM) for 1 h and then assayed for remaining activity by dilution into SMTC as described above. The remaining fractional activity values were plotted versus the ratio of Cl-NIL to DDAH1 concentrations and a linear fit of the initial points was extrapolated to find the intercept, which gives the partition ratio.[32]

In cell target validation

To compare the efficacy of DDAH1 inactivators for modification of the active site in a cultured cell environment, a competitive labeling strategy was used.[16, 22] Cultured HEK293T cells were seeded in two 6-well polystyrene plates using complete growth medium containing DMEM with 10 % FBS (Invitrogen, Carlsbad, CA) and grown to 80 % confluency. The pEF6a-DDAH-1 plasmid, which encodes an *N*-terminally myc-tagged DDAH-1, was transiently transfected into HEK293T cells using Lipofectamine 2000 (Invitrogen, Carlsbad, CA). After 24 h, spent medium was removed and the cells were each washed with 1 mL of 0.5 mL PBS at pH 7.2 (Invitrogen, Carlsbad, CA). To separate wells, the DDAH1 inactivators were added (10 μM each of Cl-NIL, Cl-NIO, Me-Cl-NIL, or Me-Cl-NIO). The compounds were allowed to incubate at 37 ºC in an atmosphere of 5 % CO_2 for 15 min before the addition of CAA-probe (110 μM), followed by an additional 10 min incubation. After treatment, cells were washed two times with PBS (1 mL) to remove inhibitors remaining in the extracellular environment and harvested in 1

mL PBS followed by centrifugation at 14000 *g* for 5 min at 4 ºC. Cell pellets were stored at – 80 ºC before analysis. The frozen cell pellets were thawed, lysed, labeled with biotin-PEO_3-azide using bioorthogonal chemistry and analyzed by two-color Western blot detection, as described below.

In cell apparent IC_{50} determination

HEK293T cells were grown, seeded, and transfected with pEF6a-DDAH-1 as described above. Stock solutions of Cl-NIL (10 mM) were diluted into complete growth medium in the cultures (1000 µL each well) to give final concentrations of 0.078, 0.156, 0.313, 0.625, 1.25, 2.5, 5, 10, 20, 40, 80, and 0 µM. The resulting cultures were subsequently incubated for 15 min at 37 ºC in an atmosphere of 5 % CO_2 before addition of CAA-probe (110 µM), followed by an additional 10 min incubation. After treatment, cells were washed two times with PBS (1 mL) to remove the media, and harvested in 1 mL PBS followed by centrifugation at 14000 *g* for 5 min at 4 ºC. Cell pellets were stored at – 80 ºC prior to analysis.

Frozen cell pellets were lysed and labeled with biotin-PEO_3-azide using bioorthogonal chemistry as described earlier.[16, 22] Briefly, cell pellets were resuspended in PB Buffer (10 mM sodium / potassium phosphate buffer at pH 8.0 containing the complete mini EDTA-free protease cocktail inhibitor (Roche, Indianapolis, IN) and Triton X-100 (1%)) and then were subjected to three cycles of vortexing, freezing in liquid N_2, and thawing at room temperature. The resulting solution was centrifuged at 14000 *g* for 5 min at 4 ºC to pellet insoluble cell debris, which was then discarded. The remaining supernatant was analyzed for total protein concentration using the Bradford assay. Biotin-PEO_3-azide was appended to alkyne functional groups in the resulting mixture using the Cu(I) catalyzed 1,3 dipolar cycloaddition reaction as follows: 25 µg total protein in 50 µL PB buffer was mixed with 0.5 µL of biotin-PEO_3-azide (2.5

mM), 0.5 μL $CuSO_4$ (50 mM), 0.5 μL tris(2-carboxyethyl)phosphine (TCEP, 50 mM) and 1.65 μL tris[(1-benzyl-1H-1,2,3-trazol-4-yl)methyl]amine (TBTA, 1.5 mM), vortexed and incubated at 25° C for 1 h. Reactions were quenched by addition of 2 × SDS loading buffer and heat inactivated at 100 °C for 10 min.

Samples were directly used for SDS-PAGE or stored at -80 °C before analysis. Two-color Western blot detection was used to detect the expression levels of DDAH1 through recognition of the genetically encoded myc-tag, and detection of any biotin-labeled proteins, as described previously.[21] Fluorescent emission images were captured using an Odyssey Infrared Imaging System (Li-Cor Biosciences, Lincoln, NE) at the Core DNA Facility (University of Texas, Austin). Fluorescence intensities (I) for both 680 nm and 800 nm channels were integrated. The response to the myc-tag (I_{680}, displayed in red) was used normalize the response to the biotin tag (I_{800}, displayed in green) for any loading differences. The resulting I_{680} values, expressed as a percentage of response to the sample with no Cl-NIL (100%), were plotted versus Cl-NIL concentration and fitted (Fluorescence Intensity (%) = 100% - (100%/(1+(IC_{50}/[Cl-NIL])^h))) to determine IC_{50} and the Hill coefficient (h).

X-ray crystallography

Prior to crystallization set-up, protein was incubated with Cl-NIL in the following mixture: 12 mg/mL purified recombinant human His_6-DDAH1 in 100 mM KCl, 100 mM potassium phosphate, pH 7.3, 10 % glycerol, 2 mM dithiothreitol, 0.7 mM Cl-NIL. At the Macromolecular Crystallography Facility (University of Texas at Austin) co-crystals were grown at 4 ˚C of the Cl-NIL:His_6-DDAH1 complex using the sitting drop method from the inactivator:enzyme mixture and 20 % PEG 3350, 0.2 M NaCl. Prior to data collection, a crystal

was transferred briefly to a drop of 20 % PEG 3350, 0.2 M NaCl, 0.1 M HEPES at pH 7.2, 10 % propylene glycol for cryoprotection. The crystal was mounted in a cryoloop (Hampton Research, Laguna Niguel, CA), flash cooled in liquid nitrogen, and mounted in the cold stream on the goniostat.

X-ray diffraction data were collected from the co-crystal at 100 K at the Advanced Light Source (ALS) beamline 5.0.3 at the Lawrence Berkeley National Laboratory. Diffraction images were processed and data reduced using HKL2000.[33] The structure of the complex was solved by molecular replacement with MOLREP[34] using the structure of human DDAH1 (PDB accession code 3I2E)[21] as the search model. Model building was carried out using Coot.[35] Refinement of models was done using PHENIX.[36] There were several rounds of refinement followed by manual rebuilding of the model. To facilitate manual rebuilding, a difference map and a $2F_o$-F_c map, σA-weighted to eliminate bias from the model[37], were prepared. A portion (5 %) of the diffraction data was set aside throughout refinement for cross-validation.[38] MolProbity[39] was used to determine areas of poor geometry and to make Ramachandran plots. The final model does not include side chain atoms for which there was no observed electron density. Coordinates and structure factors were deposited in the Protein Data Bank (accession code 6DGE).

RESULTS AND DISCUSSION

We previously reported a covalent inactivator of human DDAH1 that was designed to mimic the asymmetric dimethylarginine substrate (ADMA) of the enzyme (Figure 2): Substitution of the guanidine in the substrate with a 2-chloroacetamidine moiety resulted in an irreversible inhibitor, Cl-NIO (K_I = 1.3 μM, k_{inact} = 0.34 min^{-1}).[16] Herein, we further characterize and improve upon this strategy for designing covalent inhibitors for DDAH1. Optimizing covalent inhibitors often requires balancing non-covalent affinity and reactivity to achieve inhibition that is both potent and selective.[40] To assess both of these contributions separately, we conceptually dissected Cl-NIO into two parts and analyzed them separately: L-norvaline (L-Nva), which was expected to provide non-covalent binding affinity, and 2-chloroacetamidine (CAA), which was expected to provide the reactive group that enables covalent modification (Figure 2).[41]

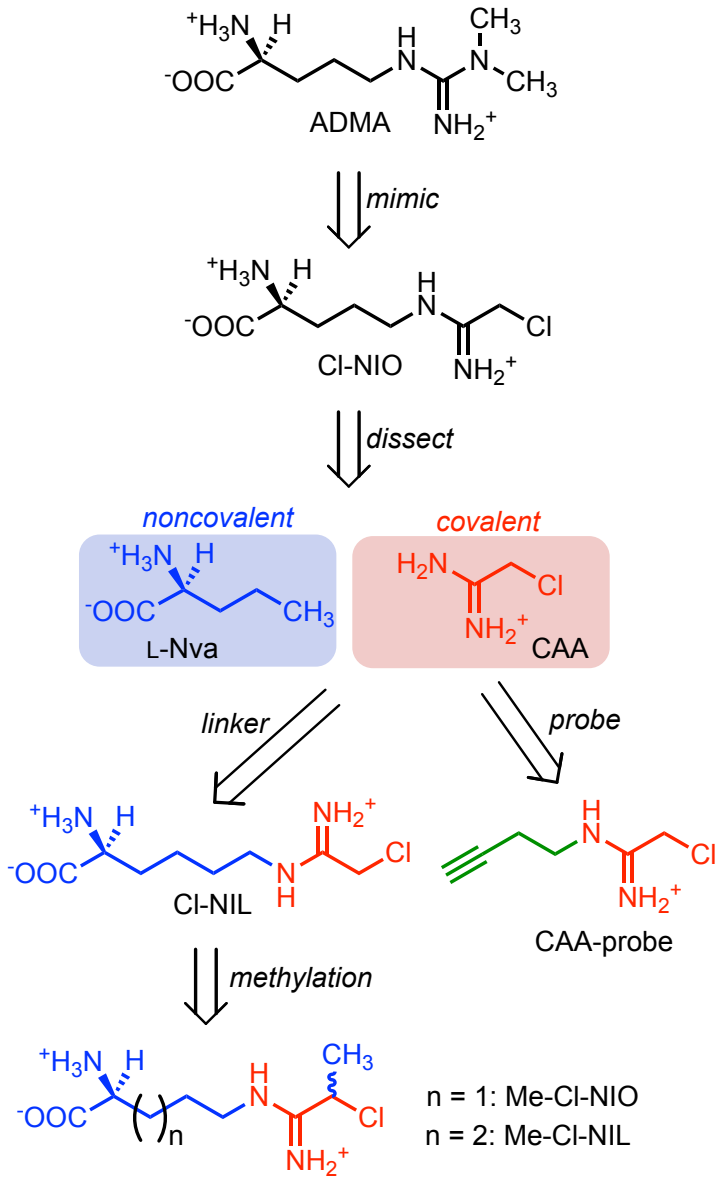

Figure 2. Structure of DDAH1 Ligands and Design Intent. A previously reported substrate (ADMA) mimic and irreversible DDAH1 inactivator (Cl-NIO) is shown with its constitutive fragments (CAA and L-Nva), an activity-based protein profiling reagent (CAA-probe), an extended-linker analog (CL-NIL) and two analogs designed to better mimic the methylation of ADMA (Me-CL-NIO, Me-CL-NIL).

L-Nva is a rapid reversible inhibitor of DDAH1 with an IC_{50} value of 1.42 ± 0.06 mM, which was used to calculate a K_i of 470 μM, assuming competitive inhibition (Figure 3, Table 1). Somewhat surprisingly, we found that the CAA reactive group also provides significant noncovalent binding to DDAH1 (K_I = 310 uM), reflecting a noncovalent affinity more potent than L-Nva (Figure 3). CAA binds approximately 10-fold more tightly to human DDAH1 than to the *Pseudomonas aeruginosa* homolog *Pa*DDAH (K_I = 3 mM), despite high active-site similarity.[41] The human DDAH1 active site is slightly smaller than that of *Pa*DDAH due to a neighboring Leu271 residue (Gly246 in *Pa*DDAH), which may improve selective interactions made with ligands to human DDAH1 and provide an opportunity for isoform selective inhibitor design.[13, 42]

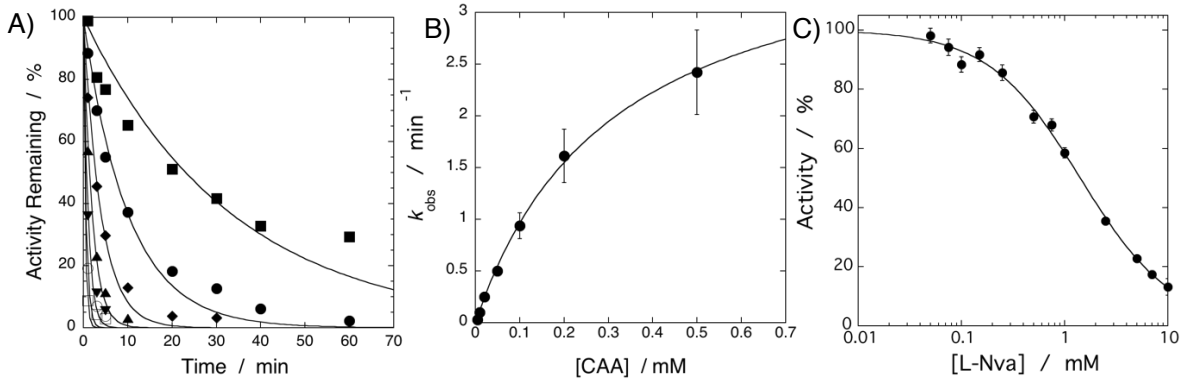

Figure 3. DDAH1 Inhibition by CAA and L-Nva. A) Preincubations of human DDAH1 with CAA (5 (■), 10(●), 20 (◆), 50 (▲), 100 (▼), 200 (○), 500 (□) μM) are diluted into excess substrate at various time points to measure activity remaining and fit as described in Experimental Procedures. B) The concentration dependence of k_{obs} values taken from A) is fit as described in Methods to determine k_{inact} (4.0 ± 0.2 min^{-1}) and K_I (310 ± 30 μM) values for CAA inactivation of DDAH1. C) Reversible L-Nva inhibition of DDAH1 was fit as described in

Methods to determine IC_{50} (1.42 ± 0.06 mM), Hill coefficient (0.97 ± 0.3) and a calculated K_i (470 ± 20 μM).

Table 1. Kinetic parameters of DDAH1 inactivation / inhibition.

Compound	k_{inact} (min^{-1})	K_I (μM)	k_{inact} / K_I ($M^{-1}s^{-1}$)
Cl-NIO[a]	0.34 ± 0.07	1.3 ± 0.6	(4.4 ± 0.3) × 10^3
CAA	4.0 ± 0.2	310 ± 30	(2.2 ± 0.3) × 10^2
L-Nva	N.A.[b]	470 ± 20[c]	N.A.
Cl-NIL	0.22 ± 0.02	0.19 ± 0.04	(1.9 ± 0.6) × 10^4
Me-Cl-NIO	N.D.[d]	N.D.	208 ± 3
Me-Cl-NIL	N.D.	N.D.	440 ± 20

[a] Values taken from reference (*16*).

[b] Not Applicable

[c] K_i value

[d] Not determined. Inactivation k_{obs} values are linear up to 32 μM inactivator.

To estimate the total noncovalent affinity afforded by both fragments, we used the relationship between Gibbs free energy and equilibrium constants, here the inhibition constants given by K_i and K_I, to calculate the free energy for binding of each fragment, added the two values, and back-calculated the resulting theoretical K_d to be approximately 150 nM, a value somewhat lower than the K_I for Cl-NIO (1.3 μM).[16] However, linking inhibitory fragments can result in affinity improvements much greater than that predicted by additive binding due to the entropic advantage of unimolecularity.[43, 44] The observation that the affinity of Cl-NIO is even poorer than just the

additive values of its constituent fragments suggests that the two fragments may not be optimally linked.

In addition to noncovalent affinity, the CAA fragment also causes irreversible inactivation of DDAH1 (k_{inact} = 4 min^{-1}) (Figure 3, Table 1). We determined the rate constant for inactivation to be > 10-fold larger than that of Cl-NIO, indicating that the fragment-sized CAA can bind in a more reactive orientation when not constrained by the tethered amino acid L-Nva moiety. As was seen with noncovalent affinity above, this analysis also suggests that the CAA and L-Nva fragments are not optimally linked to allow either their binding or reactivity to be fully realized.

These findings prompted us to alter the linker to optimize noncovalent binding affinity, so we considered changing the length between the amino acid and amidine moieties of Cl-NIO. Substrate analogs with shorter linkers between the amino acid and methylguanidine groups, such as 4124W (Figure S2), are DDAH inhibitors, but are not attacked by the active-site Cys residue.[45] Therefore, we did not shorten the linker length because reaction with Cys is required for inactivation. Other studies have shown that Arg analogs with long N^{ω}-substituents on the guanidine can be well accommodated by the human DDAH1 active site and result in reversible inhibition, as demonstrated by L-257 (Figure S2) and other analogs.[13, 46] Therefore, we anticipated that DDAH1 could accommodate compounds larger than ADMA, and synthesized a lengthened version of Cl-NIO that has a linker one additional methylene in length, N^5-(1-imino-2-chloroethyl)-L-lysine (Cl-NIL) (Figure 2).

We determined that Cl-NIL is a time- and concentration-dependent inhibitor of DDAH1, with K_I and k_{inact} values of 0.19 μM and 0.22 min^{-1}, respectively (Figure 4, Table 1). Inhibition cannot be reversed upon dilution into excess substrate, and only 1 equivalent of Cl-NIL is required to inactivate DDAH1. The longer linker was well accommodated by the enzyme,

despite being larger than the substrate ADMA, and increased the noncovalent affinity by approximately 5-fold over that of Cl-NIO. The Cl-NIL k_{inact} is similar to that of Cl-NIO, suggesting that changing the linker length, but not the position of substitution (the same position on CAA is derivatized), is not sufficient to allow the most reactive binding orientation to be achieved. Although a significant improvement in noncovalent affinity is measured, a huge gain, as is sometimes observed in fragment linking, is not achieved. The free energy difference calculated from the difference between Cl-NIO and Cl-NIL K_I values is approximately 1 kcal/mol ($\Delta\Delta G=-RT\ln(K_{I,Cl\text{-}NIL}/K_{I,Cl\text{-}NIO})$. This value is close to the 0.7 kcal/mol increase in binding due to hydrophobic interactions typically estimated for addition of a methyl group,[47] so the increase in binding affinity may be derived solely from increased hydrophobic interactions rather than allowing optimal positioning of the fragments.

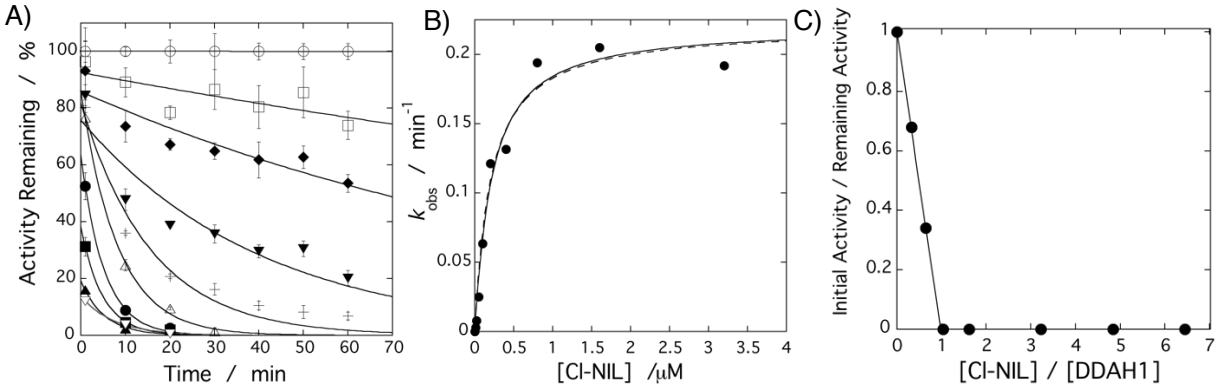

Figure 4. DDAH1 Inactivation by Cl-NIL. A) Time- and Concentration-dependent DDAH1 (0.06 μM) inactivation is observed with increasing concentrations of Cl-NIL: 0 (○), 0.0125 (□), 0.025 (◆), 0.05 (▼), 0.1 (+), 0.2 (△), 0.4 (●), 0.8 (■), 1.6 (▲), 3.2 (▽) μM in the preincubation mixture prior to dilution into excess substrate. B) A plot of k_{obs} values for inactivation derived from A) is fit by a non-linear version of the Kitz and Wilson method (dashed line, omitting points where [CL-NIL] ≤ 0.2 μM) to derive K_I (0.2 ± 0.1 μM) and k_{inact} (0.22 ± 0.02

min^{-1}) values, and is also fit by a quadratic equation (solid line, no omissions) to derive K_I (0.19 ± 0.04 μM), as described in Methods. C) A plot of the fraction of remaining DDAH1 activity at extended incubation times with increasing molar equivalents of Cl-NIL is used to determine the partition ratio (0.98 ± 0.03 equivalents of Cl-NIL : equivalents of DDAH1) for inactivation by fitting the initial three points to a linear fit and solving for the x-intercept.

In an attempt to further improve positioning of the reactive CAA moiety and to more closely mimic positioning of the substrate, N^{ω}-methylated analogs of both Cl-NIO and Cl-NIL were synthesized (Figure 2). These analogs, Me-Cl-NIO and Me-Cl-NIL, were designed to more closely mimic the dimethylated status of the substrate ADMA (Figures S3, S4, Table 1). Although both compounds were irreversible time-dependent inactivators, they had much weaker noncovalent affinity, with neither showing saturation kinetics at concentrations ≤ 30 μM. The second order inactivation rate constants (k_{inact}/K_I) for these methylated derivatives were similar to that of the CAA fragment, but 1 or 2 orders of magnitude lower than the unmethylated congeners. Methylation also lowers the non-enzymatic reactivity of these chloroacetamidines by approximately 7-fold (Figure S5). Therefore, methylation decreases the reactivity of this electrophile and likely exceeds the ability of the active site to readily accommodate substituted amidines.

It is not easy to predict how well these inactivators will gain access to the targeted cytoplasmic DDAH1 enzyme because accessibility is likely mediated by cationic amino acid transporters.[10, 48] To assay for target engagement between Cl-NIL and DDAH-1 within cultured human cells, we used an activity-based protein profiling probe consisting of the CAA fragment appended to an alkyne (CAA-probe) (Figure 2).[22] When this probe is incubated with cultured HEK293T

cells that are episomally overexpressing DDAH1 (the probe is not sensitive enough to detect endogenous DDAH1 in these cells), bioorthogonal chemistry can be used to append a biotin label to the probe and enable visualization of labeled proteins. Two color western blotting enables the separate monitoring of biotin and a myc-tag that is genetically incorporated into the expressed DDAH1. At the times and CAA-probe concentrations used herein, the only significant band detected during imaging is overexpressed DDAH1. Previously, we used this system to demonstrate target engagement of DDAH1 by Cl-NIO within cultured cells, and using the relative fluorescence of each signal, estimated an apparent cellular IC_{50} of approximately 7 μM.[16] In this case, apparent IC_{50} values provide experimental guidelines for use of these inhibitors rather than reflect the true affinity of the interaction since inhibition is both time-dependent and irreversible and will be strongly dependent on the particular experimental conditions used.

Here, we used a competition assay to detect the ability of DDAH1 inhibitors, preincubated for 15 min at 10 μM each, to prevent labeling of DDAH1 by the CAA-probe in cultured HEK293T cells, as described above (Figure 5). Both Cl-NIO and Cl-NIL effectively inhibited labeling of DDAH1 by the CAA-probe, but the methylated analogs, Me-Cl-NIO and Me-Cl-NIL did not. These results are consistent with our biochemical characterization of purified DDAH1 inhibition, which revealed the methylated analogs as much less potent inhibitors. An apparent cellular IC_{50} for Cl-NIL was determined to be 10 ± 2 μM. Even though the noncovalent affinity of Cl-NIL is approximately 5-fold more potent than Cl-NIO, this advantage is not conferred on the relative apparent cellular IC_{50} values, indicating that under these particular experimental conditions, other factors (e.g. transport or k_{inact}) may be limiting. Nonetheless, these experiments provide evidence that Cl-NIL can block active-site labeling of DDAH1 expressed within cultured cells.

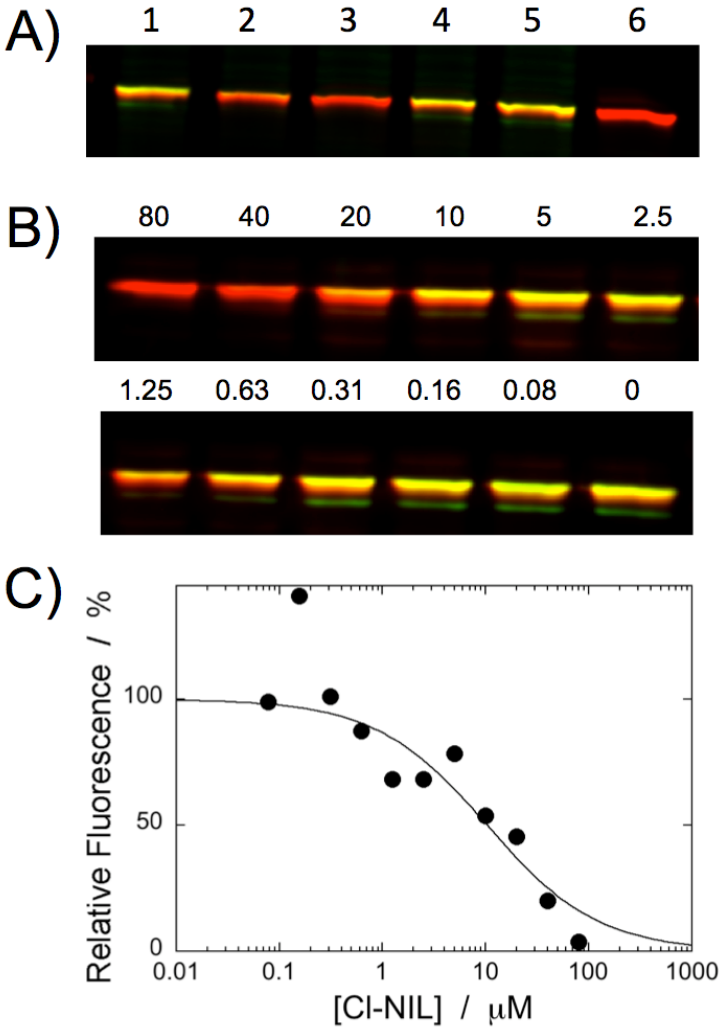

Figure 5. DDAH1 Labeling Within Cultured HEK293T Cells. A) Cultured human HEK293T cells episomally expressing myc-tagged DDAH1 were treated with 1) no inactivator, 2) Cl-NIL, 3) Cl-NIO, 4) Me-Cl-NIL, 5) Me-Cl-NIO, 6) no CAA-probe, with each inactivator treatment at 10 μM. Cell cultures were incubated for the same lengths of time, treated with CAA-probe (except for 6, which is a 'no probe' control) to label available DDAH1 active sites, and assayed as described in the Experimental Section. Two-color western blotting is used to give a red signal in response to the genetically encoded myc tag and to serve as a loading control. A green signal

is a response to DDAH1 active sites covalently labeled by CAA-Probe. Yellow indicates both signals are present. B) Cultured cells are treated with various concentrations of Cl-NIL (shown in μM above each lane) and treated as described in A). C) Using the intensity of the red fluorescent signal to normalize loading, the intensities of the green fluorescent signals are plotted for each concentration and fitted (omitting the outlier at 0.16 μM) to give an apparent in cell IC_{50} 10 ± 2 μM, with a Hill coefficient of 0.8 ± 0.2 under these experimental conditions and timeframe.

One potential off-target of particular interest is arginase, because the substrate of this enzyme (L-Arg) is quite similar to that of DDAH1 (ADMA), and because the activity of arginase can also impact nitric oxide production through L-Arg depletion.[49] Using purified enzyme, we determined that Cl-NIL is not a very effective inhibitor of human dimanganese (II) arginase, and measured an IC_{50} value of 20 mM, which represents >100,000-fold selectivity (based on comparison of IC_{50} and K_I values) (Figure S6). Likely the ω-carbon and chloro substituent in Cl-NIL prevents coordination to, or sufficient proximity to, the metal center, as is seen with the endogenous L-Arg substrate during turnover.[49] Off-target inhibition by covalent inactivators can lead to cytotoxicity, so we also evaluated the cell viability of cultured HEK293T cells and found the concentration at half maximum for cell killing to be 118 ± 2 μM, which provides a wide window between the concentrations effective for blocking the active-site of DDAH1 and the concentrations that are cytotoxic (Figure S7).

Because Cl-NIL appears to be a promising tool for the study of DDAH1, we chose this inhibitor for structural determination. A 1.9 Å resolution X-ray co-crystal structure of the Cl-NIL:DDAH1 complex was determined (Table 2). The overall protein fold is very similar to that

of product (L-citrulline)-bound DDAH1 reported earlier (2JAI), with a RMSD between 271 α-carbon atom pairs of 0.5 Å.[13] However, the active sites are different. The Fo-Fc omit map, omitting the ligand and Cys274, shows strong electron density at the active site of DDAH1, consistent with active site binding of a ligand, and continuous density is observed between this bound ligand and the active-site Cys274 residue (Figure 6). The covalent adduct can be well fit by a modification of the active site Cys thiol with N^5-(1-iminoethyl)-L-lysine (Cl-NIL after loss of the chloro substituent), covalently linked through a thioether bond with the ω-carbon of the amidine. This adduct has the same thioether connection observed when *P. aeruginosa* DDAH is inactivated by the CAA fragment, suggesting similar inactivation mechanisms.[41] The longer linker found in Cl-NIL can be accommodated with only rotomeric changes in comparison to a DDAH1 structure determined with bound product, with only two obvious changes apart from Cys modification. First, the catalytic His173 residue is rotated to create extra volume in the active-site cavity. A similar rotation is seen when DDAH1 binds Arg-based inhibitors bearing long N^{ω}-substitutents, and appears to be a general way for this enzyme to accommodate larger ligands.[2, 46] The second change is instead seen in the ligand where the extreme ends of the inactivator (the amidine ω-nitrogen and the amino acid moiety) bind in identical positions to that of product, but the linker region in between bows out like an accordion to accommodate the extra methylene group (Figure 6). A structural consequence of this bowing is loss of one of the two potential H-bonds formed between the amidine nitrogens and the active-site Asp79. In comparison, a bidentate interaction is observed between the urea nitrogens of the product L-citrulline and Asp79, presumably through two H-bonds. This observation suggests that if further optimization of Cl-NIL is pursued, strategies to recapture this second interaction with Asp79 may lead to further increases in potency.

Table 2. Crystallographic Data

	CL-NIL:DDAH1
Space group	P41
Cell constants	a=b=55.2, c=89.5 Å
Resolution (Å)[a]	50.-1.91 (1.94-1.91)
R_{merge} (%)	0.072 (0.500)
$<I/\sigma_I>$	10.3 (3.4)
Completeness (%)	100.0 (100.0)
Unique reflections	20,872
Redundancy	7.5 (6.7)
# of residues	275
# of protein atoms	2024
# of ligand atoms	13
# of solvent atoms	83
$R_{working}$	0.215
R_{free}	0.251
Average B factor for protein atoms ($Å^2$)	24.7
Average B factor for ligand atoms ($Å^2$)	22.0
Average B factor for solvent atoms ($Å^2$)	24.2
rms deviation from ideality	
bonds (Å)	0.004
angles (°)	0.864
Ramachandran plot	
% of residues in favored region	96.7
% of residues in additional allowed region	3.3

[a] Values in parentheses correspond to highest resolution shell

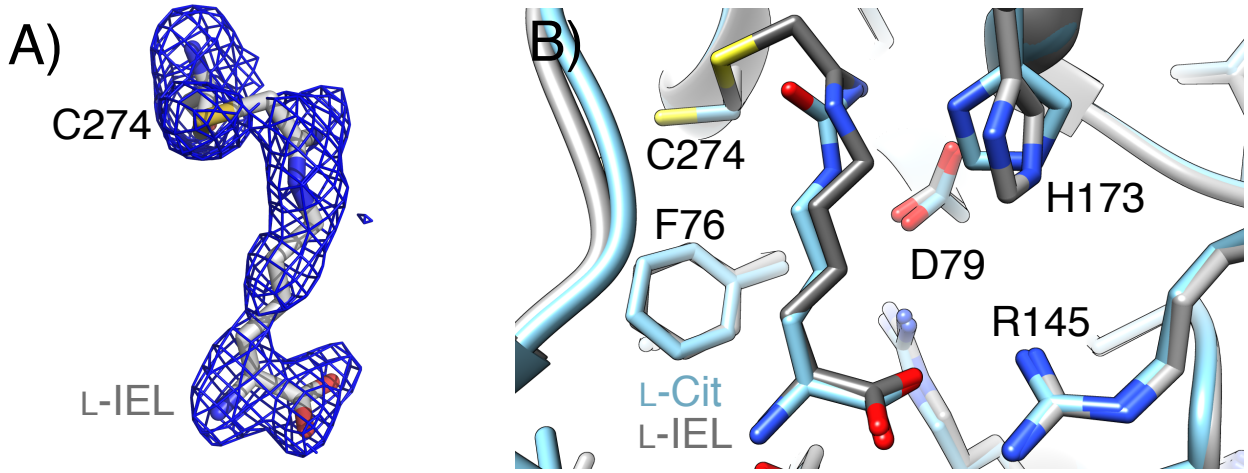

Figure 6. Structural Analysis of DDAH1 Inactivation by Cl-NIL. A) After inactivation of DDAH1 by Cl-NIL, the Fo-Fc omit map for Cys274 and the covalently-bound ligand is shown in blue, contoured at 2σ. There is continuous density from Cys274 to the covalently bound inhibitor. B) X-Ray structures of the Cl-NIL:DDAH1 complex (grey) and the L-citrulline (L-Cit):DDAH1 complex (light blue, from PDB accession code 2JAI) are superimposed with the ligands of each centered in the image. Loss of chloride from Cl-NIL results in the covalent attachment of N^5-(1-iminoethyl)-L-lysine (L-IEL). This comparison highlights a covalent linkage formed between Cys274 and L-IEL, one-fewer H-bond between L-IEL and Asp79 (center, back) in comparison with L-Cit, and rotation of His173 to accommodate the extended length of the inactivator. In both panels, heteroatoms are colored in blue, red or yellow, for nitrogen, oxygen or sulfur, respectively.

SUMMARY AND CONCLUSIONS

The origins of noncovalent binding affinity and reactivity were studied for the DDAH1 inactivator Cl-NIO by dissecting the compound into two fragments expected to correspond

roughly to the "binding" fragment (L-Nva) and the "reactive" fragment (CAA). Surprisingly, the CAA fragment provided more noncovalent affinity than the other fragment, and the additive properties of each suggested that their linkage did not enable the full potential of either fragment to be expressed in Cl-NIO. In response, we used a longer linker in Cl-NIL, which was not an obvious modification since Cl-NIO more closely resembles the size of the enzyme's substrate. Despite its larger size, Cl-NIL is well accommodated at the active-site through rotation of a catalytic His173 residue, which seems to be a common method for DDAH1 to accommodate larger ligands, and by a bowing out of the ligand with loss of one of potential H-bond from the amidine to an acid site Asp79 residue. Although the longer linker still does not allow the fragments to achieve the optimal binding, the observed ligand:enzyme structure does suggest possible ways to further improve noncovalent affinity. Regardless, to the best of our knowledge, the K_I of Cl-NIL is more potent than any K_I, K_i or IC_{50} value reported for extant DDAH1 inhibitors.[20] In addition, the k_{inact}/K_I value (1.9×10^4 $M^{-1}s^{-1}$) exceeds the catalytic efficiency of DDAH1 for its endogenous substrate ADMA ($k_{cat}/K_M = 1.6 \times 10^2$ $M^{-1}s^{-1}$) by approximately 100-fold.[23] We would have not undertaken this linker modification unless prompted by the separate analysis of the constitutive fragments. The type of covalent inhibition by Cl-NIL is likely best classified[40] as either affinity labeling, due to the inherent reactivity of the CAA fragment, or as mechanism-based inactivation, through comparison to mechanistic studies that characterized the inactivation of the homologous enzyme protein arginine deiminase by the related compound Cl-amidine.[50] Cl-NIL is selective for inhibition of DDAH1 instead of arginase, and shows little or no toxicity to cultured HEK293T cells at concentrations used to validate target engagement of cytoplasmic DDAH1. Therefore, Cl-NIL is a promising biochemical tool for the study of DDAH1-related pathways. Dissecting a ligand to parse the contributions of its constituent

fragments has proved helpful in the past to characterize interactions between ligand and protein,[43, 44] and has proved useful here to optimize the most potent DDAH1 inactivator reported to date.

ASSOCIATED CONTENT

Supporting Information.

The following files are available free of charge:

Supporting figures for synthesis, DDAH1 inhibitors, time-dependent DDAH1 inactivation by Me-Cl-NIL, Me-Cl-NIL, nonenzymic reactivity of substituted chloroacetamidines, inhibition of arginase by Cl-NIL, and HEK293T cytotoxicity assay for Cl-NIL (PDF).

AUTHOR INFORMATION

Corresponding Author

*E-mail: walt.fast@austin.utexas.edu (W.F.).

ORCID

Walter Fast: 0000-0001-7567-2213

NOTES

The authors declare no competing financial interest.

ACKNOWLEDGEMENT

For purified human arginase, we thank Everett Stone (University of Texas, Austin). This work was supported in part by grants from the National Institutes of Health (GM69754) and the Robert A. Welch Foundation (F-1572). A.T. acknowledges a postdoctoral fellowship from the National Institutes of Health (1K12 GM102745). Additional assistance was provided by the Macromolecular Crystallography Facility, with financial support from the College of Natural Sciences, the Office of the Executive Vice President and Provost, and the Institute for Cellular and Molecular Biology at the University of Texas at Austin. The Berkeley Center for Structural Biology is supported in part by the National Institutes of Health, National Institute of General Medical Sciences, and the Howard Hughes Medical Institute. The Advanced Light Source is supported by the Director, Office of Science, Office of Basic Energy Sciences, of the U.S. Department of Energy under Contract No. DE-AC02-05CH11231.

REFERENCES

1. Alderton, W. K., Cooper, C. E., and Knowles, R. G. (2001) Nitric oxide synthases: structure, function and inhibition, *Biochem. J. 357*, 593-615.

2. Leiper, J., and Nandi, M. (2011) The therapeutic potential of targeting endogenous inhibitors of nitric oxide synthesis, *Nat. Rev. Drug Discov. 10*, 277-291.

3. Shirakawa, T., Kako, K., Shimada, T., Nagashima, Y., Nakamura, A., Ishida, J., and Fukamizu, A. (2011) Production of free methylarginines via the proteasome and autophagy pathways in cultured cells, *Mol. Med. Rep. 4*, 615-620.

4. Vallance, P., Leone, A., Calver, A., Collier, J., and Moncada, S. (1992) Accumulation of an endogenous inhibitor of nitric oxide synthesis in chronic renal failure, *Lancet 339*, 572-575.

5. Cardounel, A. J., Cui, H., Samouilov, A., Johnson, W., Kearns, P., Tsai, A. L., Berka, V., and Zweier, J. L. (2007) Evidence for the pathophysiological role of endogenous methylarginines in regulation of endothelial NO production and vascular function, *J. Biol. Chem. 282*, 879-887.

6. Babu, B. R., Frey, C., and Griffith, O. W. (1999) L-Arginine binding to nitric-oxide synthase. The role of H-bonds to the nonreactive guanidinium nitrogens, *J. Biol. Chem. 274*, 25218-25226.

7. MacAllister, R. J., Whitley, G. S., and Vallance, P. (1994) Effects of guanidino and uremic compounds on nitric oxide pathways, *Kidney Int. 45*, 737-742.

8. Olken, N. M., Osawa, Y., and Marletta, M. A. (1994) Characterization of the inactivation of nitric oxide synthase by N^G-methyl-L-arginine: evidence for heme loss, *Biochemistry 33*, 14784-14791.

9. Boer, R., Ulrich, W. R., Klein, T., Mirau, B., Haas, S., and Baur, I. (2000) The inhibitory potency and selectivity of arginine substrate site nitric-oxide synthase inhibitors is solely determined by their affinity toward the different isoenzymes, *Mol. Pharmacol. 58*, 1026-1034.

10. Kittel, A., and Maas, R. (2014) Pharmacology and clinical pharmacology of methylarginines used as inhibitors of nitric oxide synthases, *Curr. Pharm. Des. 20*, 3530-3547.

11. Caplin, B., and Leiper, J. (2012) Endogenous nitric oxide synthase inhibitors in the biology of disease: markers, mediators, and regulators?, *Arterioscler. Thromb. Vasc. Biol. 32*, 1343-1353.

12. Hu, X., Atzler, D., Xu, X., Zhang, P., Guo, H., Lu, Z., Fassett, J., Schwedhelm, E., Boger, R. H., Bache, R. J., and Chen, Y. (2011) Dimethylarginine dimethylaminohydrolase-1 is the critical enzyme for degrading the cardiovascular risk factor asymmetrical dimethylarginine, *Arterioscler. Thromb. Vasc. Biol. 31*, 1540-1546.

13. Leiper, J., Nandi, M., Torondel, B., Murray-Rust, J., Malaki, M., O'Hara, B., Rossiter, S., Anthony, S., Madhani, M., Selwood, D., Smith, C., Wojciak-Stothard, B., Rudiger, A., Stidwill, R., McDonald, N. Q., and Vallance, P. (2007) Disruption of methylarginine metabolism impairs vascular homeostasis, *Nat. Med. 13*, 198-203.

14. Wang, Z., Lambden, S., Taylor, V., Sujkovic, E., Nandi, M., Tomlinson, J., Dyson, A., McDonald, N., Caddick, S., Singer, M., and Leiper, J. (2014) Pharmacological inhibition of DDAH1 improves survival, haemodynamics and organ function in experimental septic shock, *Biochem. J. 460*, 309-316.

15. Pullamsetti, S. S., Savai, R., Dumitrascu, R., Dahal, B. K., Wilhelm, J., Konigshoff, M., Zakrzewicz, D., Ghofrani, H. A., Weissmann, N., Eickelberg, O., Guenther, A., Leiper, J., Seeger, W., Grimminger, F., and Schermuly, R. T. (2011) The role of dimethylarginine dimethylaminohydrolase in idiopathic pulmonary fibrosis, *Sci. Trans. Med. 3*, 87ra53.

16. Wang, Y., Hu, S., Gabisi, A. M., Jr., Er, J. A., Pope, A., Burstein, G., Schardon, C. L., Cardounel, A. J., Ekmekcioglu, S., and Fast, W. (2014) Developing an irreversible inhibitor of human DDAH-1, an enzyme upregulated in melanoma, *ChemMedChem 9*, 792-797.

17. Sikora, A. G., Gelbard, A., Davies, M. A., Sano, D., Ekmekcioglu, S., Kwon, J., Hailemichael, Y., Jayaraman, P., Myers, J. N., Grimm, E. A., and Overwijk, W. W. (2010) Targeted inhibition of inducible nitric oxide synthase inhibits growth of human melanoma in vivo and synergizes with chemotherapy, *Clin. Cancer Res. 16*, 1834-1844.

18. Ekmekcioglu, S., Ellerhorst, J. A., Prieto, V. G., Johnson, M. M., Broemeling, L. D., and Grimm, E. A. (2006) Tumor iNOS predicts poor survival for stage III melanoma patients, *Int. J. Cancer 119*, 861-866.

19. Reddy, K. R. K., Dasari, C., Duscharla, D., Supriya, B., Ram, N. S., Surekha, M. V., Kumar, J. M., and Ummanni, R. (2018) Dimethylarginine dimethylaminohydrolase-1 (DDAH1) is frequently upregulated in prostate cancer, and its overexpression conveys tumor growth and angiogenesis by metabolizing asymmetric dimethylarginine (ADMA), *Angiogenesis 21*, 79-94.

20. Murphy, R. B., Tommasi, S., Lewis, B. C., and Mangoni, A. A. (2016) Inhibitors of the Hydrolytic Enzyme Dimethylarginine Dimethylaminohydrolase (DDAH): Discovery, Synthesis and Development, *Molecules 21*, E615.

21. Wang, Y., Monzingo, A. F., Hu, S., Schaller, T. H., Robertus, J. D., and Fast, W. (2009) Developing dual and specific inhibitors of dimethylarginine dimethylaminohydrolase-1 and nitric oxide synthase: toward a targeted polypharmacology to control nitric oxide, *Biochemistry 48*, 8624-8635.

22. Wang, Y., Hu, S., and Fast, W. (2009) A click chemistry mediated in vivo activity probe for dimethylarginine dimethylaminohydrolase, *J. Am. Chem. Soc. 131*, 15096-15097.

23. Hong, L., and Fast, W. (2007) Inhibition of human dimethylarginine dimethylaminohydrolase-1 by *S*-nitroso-L-homocysteine and hydrogen peroxide. Analysis, quantification, and implications for hyperhomocysteinemia, *J. Biol. Chem. 282*, 34684-34692.

24. Linsky, T. W., and Fast, W. (2012) Discovery of structurally-diverse inhibitor scaffolds by high-throughput screening of a fragment library with dimethylarginine dimethylaminohydrolase, *Bioorg. Med. Chem. 20*, 5550-5558.

25. Linsky, T., and Fast, W. (2011) A continuous, fluorescent, high-throughput assay for human dimethylarginine dimethylaminohydrolase-1, *J. Biomol. Screen. 16*, 1089-1097.

26. Stone, E. M., and Fast, W. (2005) A continuous spectrophotometric assay for dimethylarginine dimethylaminohydrolase, *Anal. Biochem. 343*, 335-337.

27. Copeland, R. A. *Evaluation of enzyme inhibitors in drug discovery*, Wiley-Interscience, Hoboken, N.J, 2005.

28. Williams, J. W., and Morrison, J. F. (1979) The kinetics of reversible tight-binding inhibition, *Method. Enzymol. 63*, 437-467.

29. Kitz, R., and Wilson, I. B. (1962) Esters of methanesulfonic acid as irreversible inhibitors of acetylcholinesterase, *J. Biol. Chem. 237*, 3245-3249.

30. Knipp, M., and Vasak, M. (2000) A colorimetric 96-well microtiter plate assay for the determination of enzymatically formed citrulline, *Anal. Biochem. 286*, 257-264.

31. Cheng, Y., and Prusoff, W. H. (1973) Relationship between the inhibition constant (K1) and the concentration of inhibitor which causes 50 per cent inhibition (I50) of an enzymatic reaction, *Biochem. Pharmacol. 22*, 3099-3108.

32. Silverman, R. B. (1995) Mechanism-based enzyme inactivators, *Method. Enzymol. 249*, 240-283.

33. Otwinowski, Z., and Minor, W. (1997) Processing of X-ray diffraction data collected in oscillation mode, *Method. Enzymol. 276*, 307-326.

34. Vagin, A., and Teplyakov, A. (2010) Molecular replacement with MOLREP, *Acta Crystallograph. D, Biol. Crystallograph. 66*, 22-25.

35. Emsley, P., Lohkamp, B., Scott, W. G., and Cowtan, K. (2010) Features and development of Coot, *Acta Crystallograph. D, Biol. Crystallograph. 66*, 486-501.

36. Adams, P. D., Afonine, P. V., Bunkoczi, G., Chen, V. B., Davis, I. W., Echols, N., Headd, J. J., Hung, L. W., Kapral, G. J., Grosse-Kunstleve, R. W., McCoy, A. J., Moriarty, N. W., Oeffner, R., Read, R. J., Richardson, D. C., Richardson, J. S., Terwilliger, T. C., and Zwart, P. H. (2010) PHENIX: a comprehensive Python-based system for macromolecular structure solution, *Acta Acta Crystallograph. D, Biol. Crystallograph. 66*, 213-221.

37. Read, R. J. (1986) Improved Fourier coefficients for maps using phases from partial structures with errors., *Acta. Crystallograph. A 42*, 140-149.

38. Brunger, A. T. (1993) Assessment of phase accuracy by cross validation: the free R value. Methods and applications, *Acta Crystallograph. D, Biol. Crystallograph. 49*, 24-36.

39. Davis, I. W., Leaver-Fay, A., Chen, V. B., Block, J. N., Kapral, G. J., Wang, X., Murray, L. W., Arendall, W. B., 3rd, Snoeyink, J., Richardson, J. S., and Richardson, D. C. (2007) MolProbity: all-atom contacts and structure validation for proteins and nucleic acids, *Nucleic Acids Res. 35*, W375-383.

40. Tuley, A., and Fast, W. (2018) The Taxonomy of Covalent Inhibitors, *Biochemistry, 57,* 3326-3337.

41. Stone, E. M., Schaller, T. H., Bianchi, H., Person, M. D., and Fast, W. (2005) Inactivation of two diverse enzymes in the amidinotransferase superfamily by 2-chloroacetamidine: dimethylargininase and peptidylarginine deiminase, *Biochemistry 44*, 13744-13752.

42. Murray-Rust, J., Leiper, J., McAlister, M., Phelan, J., Tilley, S., Santa Maria, J., Vallance, P., and McDonald, N. (2001) Structural insights into the hydrolysis of cellular nitric oxide synthase inhibitors by dimethylarginine dimethylaminohydrolase, *Nat. Struct. Biol. 8*, 679-683.

43. Jencks, W. P. (1981) On the attribution and additivity of binding energies, *Proc. Nat. Acad. Sci. U.S.A. 78*, 4046-4050.

44. Nakamura, C. E., and Abeles, R. H. (1985) Mode of interaction of beta-hydroxy-beta-methylglutaryl coenzyme A reductase with strong binding inhibitors: compactin and related compounds, *Biochemistry 24*, 1364-1376.

45. MacAllister, R. J., Parry, H., Kimoto, M., Ogawa, T., Russell, R. J., Hodson, H., Whitley, G. S., and Vallance, P. (1996) Regulation of nitric oxide synthesis by dimethylarginine dimethylaminohydrolase, *Br. J. Pharmacol. 119*, 1533-1540.

46. Lluis, M., Wang, Y., Monzingo, A. F., Fast, W., and Robertus, J. D. (2011) Characterization of C-alkyl amidines as bioavailable covalent reversible inhibitors of human DDAH-1, *ChemMedChem 6*, 81-88.

47. Leung, C. S., Leung, S. S., Tirado-Rives, J., and Jorgensen, W. L. (2012) Methyl effects on protein-ligand binding, *J. Med. Chem. 55*, 4489-4500.

48. Closs, E. I., Basha, F. Z., Habermeier, A., and Forstermann, U. (1997) Interference of L-arginine analogues with L-arginine transport mediated by the y^+ carrier hCAT-2B, *Nitric Oxide 1*, 65-73.

49. Christianson, D. W. (2005) Arginase: structure, mechanism, and physiological role in male and female sexual arousal, *Acc. Chem. Res. 38*, 191-201.

50. Knuckley, B., Causey, C. P., Pellechia, P. J., Cook, P. F., and Thompson, P. R. (2010) Haloacetamidine-based inactivators of protein arginine deiminase 4 (PAD4): evidence that general acid catalysis promotes efficient inactivation, *ChemBioChem 11*, 161-165.

TOC Graphic for

Dissection, Optimization and Structural Analysis of

a Covalent Irreversible DDAH1 Inhibitor

Gayle Burstein-Teitelbaum, Joyce A.V. Er, Arthur F. Monzingo, Alfred Tuley, Walter Fast*